

FATIGUE ANALYSIS OF ORTHOTROPIC HIGHWAY BRIDGE DECKS

Kornél Kiss¹, Ernő Székely² and László Dunai³

Technical University of Budapest, Department of Steel Structures

1111 Budapest, Műegyetem rkp. 5-7, Hungary

SUMMARY

A FEM-based *integrated stress analysis and fatigue design* is introduced for orthotropic bridge decks. The 3D plate/shell model of a large part of the bridge includes the deck plate, cross beams, ribs and part of the main girder webs. This model can consider the local membrane- and bending actions as well as the main girder effect, warping, shear lag, and the interaction of structural elements. The stress spectra obtained from this model are used to perform fatigue analysis based on S-N curves (*Wöhler curves*).

A second level of modeling can be developed for weld details made up of 2D plane strain elements. Considering the stress concentrations due to weld geometry and flaws allows the use of a direct fracture mechanics approach to fatigue design by computing the rate of crack propagation and determining the critical crack length from the residual strength diagram. The global model used with S-N curve-based fatigue assessment is explained in this paper, *illustrated by real bridge structure*, according to Eurocode 3 recommendations.

Keywords: orthotropic decks, S-N curves (Wöhler curves), 3D plate/shell models, geometric stress concentration, damage equivalent stress range, linear damage accumulation

1. INTRODUCTION

The complex stress field in the components of an orthotropic highway deck is the result of three actions. The stresses arising from the "main girder effect" are called the *primary* stresses. These membrane stresses are due to the bending of the main girder, when the orthotropic deck is simply considered as the upper flange. Taking into account the orthogonal anisotropy of the deck, and the distribution of the loads corresponding to the rigidities of the ribs and crossbeams, *secondary* stresses can be computed. Finally, the local bending of the isotropic plate elements under direct wheel loading causes *tertiary* stresses. Building a FE model using 3D plate/shell elements with six degrees of freedom per node may allow the study of all three actions. In certain places, such as in the vicinity of crossbeam/rib connections, where copeholes may be present, the density of the

¹Ph.D. Student

²Fifth Year Student, Faculty of Civil Engineering, TU Budapest

³Associate Professor

mesh should be adequate to allow the study of stress concentrations due to the overall geometry of the detail. The above described *modern stress analysis* must be joined by an *advanced fatigue assessment* to form an integrated system. The fatigue assessment recommended by Eurocode 3 is an up-to-date method based on S-N curves, which is suitable for this purpose. To show how the proposed fatigue design system can be used in a real design situation, an orthotropic bridge deck is analyzed in Part 3.

2. REVIEW OF FATIGUE ASSESSMENT METHODS

2.1 General

For fatigue problems that belong to the high cycle fatigue regime (HCF), with a long period of stable crack growth due to stress ranges well below the yield limit, the *stress-life approach* is the most widely used. This approach was introduced more than a century ago, and it is still the best known among the designers, (Bannantine, 1990, Forsyth, 1969). The *linear elastic fracture mechanics (LEFM) approach* has been developed more recently, and it may be used in fail-safe or damage tolerant design in the HCF regime (Davoli, 1997, Kiss, 1997, Maddox, 1991). In the field of low cycle fatigue (LCF), when large plastic strains occur, the *strain-life approach* may prove more useful. Only the first approach is explained here.

2.2 Stress-life approach

The design codes specify classification tables for different details and different modes of fatigue cracking, based on their fatigue strength, (ENV 1991-3, 1993). *Design S-N curves* are given for each category, where the design value of fatigue strength *DS* is plotted against the number of repetitions *N*, as straight lines in a log-log scale (see S-N curves of Eurocode 3 on Fig. 2.1):

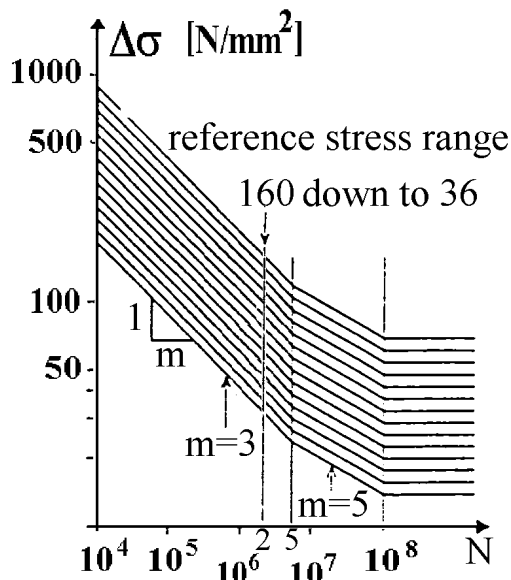


Fig. 2.1 S-N curves

$$N = \frac{A}{\Delta\sigma^m} \quad (1)$$

The maximum constant amplitude stress range that may be repeated *N* times before fracture occurs is called the *fatigue strength* of the detail. From the other point of view: for a specific constant amplitude stress history with a given stress range, the number of repetitions until fracture is called the *fatigue life*. The value of *A* and *m* depends on the classification. Stress ranges should be computed elastically, geometric stress concentrations and secondary effects (joint fixity, shear lag, etc.) must be taken into account. S-N curves by themselves could be used for constant amplitude stress histories only. In reality, however, the stress histories

of details in a bridge structure experience *variable amplitude* stress histories. Engineers may use two methods to deal with the effects of variable amplitude: using equivalent

constant amplitude stress ranges (simplified method) or using linear damage accumulation. In the following, only the pertaining Eurocode 3 rules and recommendations will be explained.

2.2.1 Fatigue load models defined by Eurocode 3

The ENV 1991-3 (1993) describes five different fatigue load models. Fatigue load models 1, 2 and 3 are intended to be used to determine the maximum and minimum stresses resulting from the possible load arrangements on the bridge of any of these models; in many cases, only the algebraic difference between these stresses is used. Fatigue load models 4 and 5 are intended to be used to determine stress range spectra resulting from the passage of lorries on the bridge.

In Part 3, fatigue load model 3 will be used to perform the simplified fatigue analysis and fatigue load model 4 will be used for the cumulative damage-based assessment.

2.2.2 Fatigue load model 3 (Single vehicle model)

This model consists of four axles, each of them having two identical wheels 2.00 meters apart. The axle spacings are: 1.20 m, 6.00 m, 1.20 m. The weight of each axle is 120 kN and the contact area of each wheel is a $0.40 \times 0.40 \text{ m}^2$ square. The maximum and minimum stresses and the stress ranges, i.e. their algebraic difference, resulting from the longitudinal and transversal locations are calculated.

2.2.3 Fatigue load model 4 (Set of "standard" lorries)

This model consists of sets of standard lorries having together effects equivalent to those of typical traffic on European roads. This model, based on five standard lorries is a simulated traffic, deemed to produce fatigue damages equivalent to those due to a real traffic of the corresponding traffic category. The number of lorries per year and per slow lane for the traffic categories can be found in Tab. 4.6 of ENV 1991-3 (1993). The set of lorries appropriate for the predicted traffic mixes for the route are defined in Tab. 4.8, and the definition of wheels and axles can be found in Tab. 4.9 of the same document. (Three types of wheels are defined: "A", "B" and "C". Axle spacing, axle wheel types (contact areas) and axle loads are different for each standard lorry.)

2.2.4 Using damage equivalent constant amplitude stress ranges

In this case, a constant amplitude stress range is computed, that causes similar damage as the variable amplitude stress range in question. According to ENV 1993-2 (1996) Chapter 9, the *fatigue criterion* is:

$$\gamma_{Ff} \Delta \sigma_{E2} \leq \Delta \sigma_c / \gamma_{Mf} , \quad (2)$$

where $\Delta \sigma_{E2}$ is the equivalent stress range for 2 million cycles, $\Delta \sigma_c$ is the reference value of the fatigue strength at 2 million cycles for the relevant detail category, γ_{Ff} is the partial safety factor for fatigue loading, and γ_{Mf} is the partial safety factor for fatigue strength. The equivalent stress range is obtained by the following formula:

$$\Delta \sigma_{E2} = \lambda \Phi_2 \Delta \sigma_p , \quad (3)$$

where DS_p is the reference stress range, I is the damage equivalence factor, and F_2 is the equivalent impact factor.

2.2.5 Using Miner's rule

Fatigue is a highly non-linear process, the degree of non-linearity is especially severe for small stress ranges. However, the *linear damage rule* is very simple, and can be used in everyday calculations. The method devised by *Palmgren* and *Miner* is the following:

1. First, the variable amplitude stress history is separated into a series of constant amplitude stress histories, and the stress spectrum for the given loading event is calculated.
2. Next, assuming that the effect of the original variable amplitude stress history is the same as the combined effects of all the component constant amplitude stress histories, total damage D is calculated as follows:

$$D = \sum_i D_i = \sum_i \frac{n_i}{N_i} \quad (4)$$

In this formula, n_i is the number of applied repetitions of damaging stress range DS_i in a *design spectrum*, and N_i is the *fatigue life* that corresponds to this stress range. Failure by fatigue occurs, when $D \geq 1.0$.

3. FATIGUE ASSESSMENT OF A HIGHWAY BRIDGE DECK

The bridge selected for the illustration of the fatigue design system described in this paper is a box girder bridge to be built over the Danube in Budapest, between Pest and the Csepel island. Construction will start at the end of 1998. The upper flange of the box is an orthotropic plate, with closed trapezoidal ribs running longitudinally. Two fatigue analyses are carried out for the weld connecting the ribs to the deck plate: one according to the equivalent stress range, and one according to Miner's rule.

3.1 The structural model

A section of the bridge deck was modeled by plate/shell elements with six degrees of freedom per node. The model includes the deck plate and the longitudinal trapezoidal ribs, six cross girders (web and lower flange), and the upper part of the webs of the main box girder. The structure is continuously supported along the main girder webs. This means that the main girder effect is ignored. The view of the model can be seen on Fig. 3.1. The top picture shows the deck plate, the trapezoidal ribs are in the middle, and the cross beams and the upper parts of the box girder webs are in the bottom. Note the density of the mesh around one part of the deck, where the wheel loads were applied.

3.2 Load model and stress analysis

First, fatigue load model 3 was placed in 9 different locations on the deck, in order to find the highest tensile (+) and compressive (-) stresses (s_{max} and s_{min}) occurring in the weld connecting the ribs to the deck plate. One of the 8 wheels was defined as a distrib-

uted load acting on the contact area, the others were represented by concentrated forces, to simulate their effect on the stresses at the first wheel. Positions 1...3 were between two cross girders, Positions 4...6 right above a cross girder, and Positions 7...9 next to a cross girder. The positions in each set varied laterally with respect to the rib axis. The resulting extreme fiber stresses in the rib walls next to the welds (perpendicular to the weld) are summarized in Tab. 3.1. Stresses occurring at the interior side of the rib wall are placed in parentheses. Stresses computed at the concentrated forces were ignored.

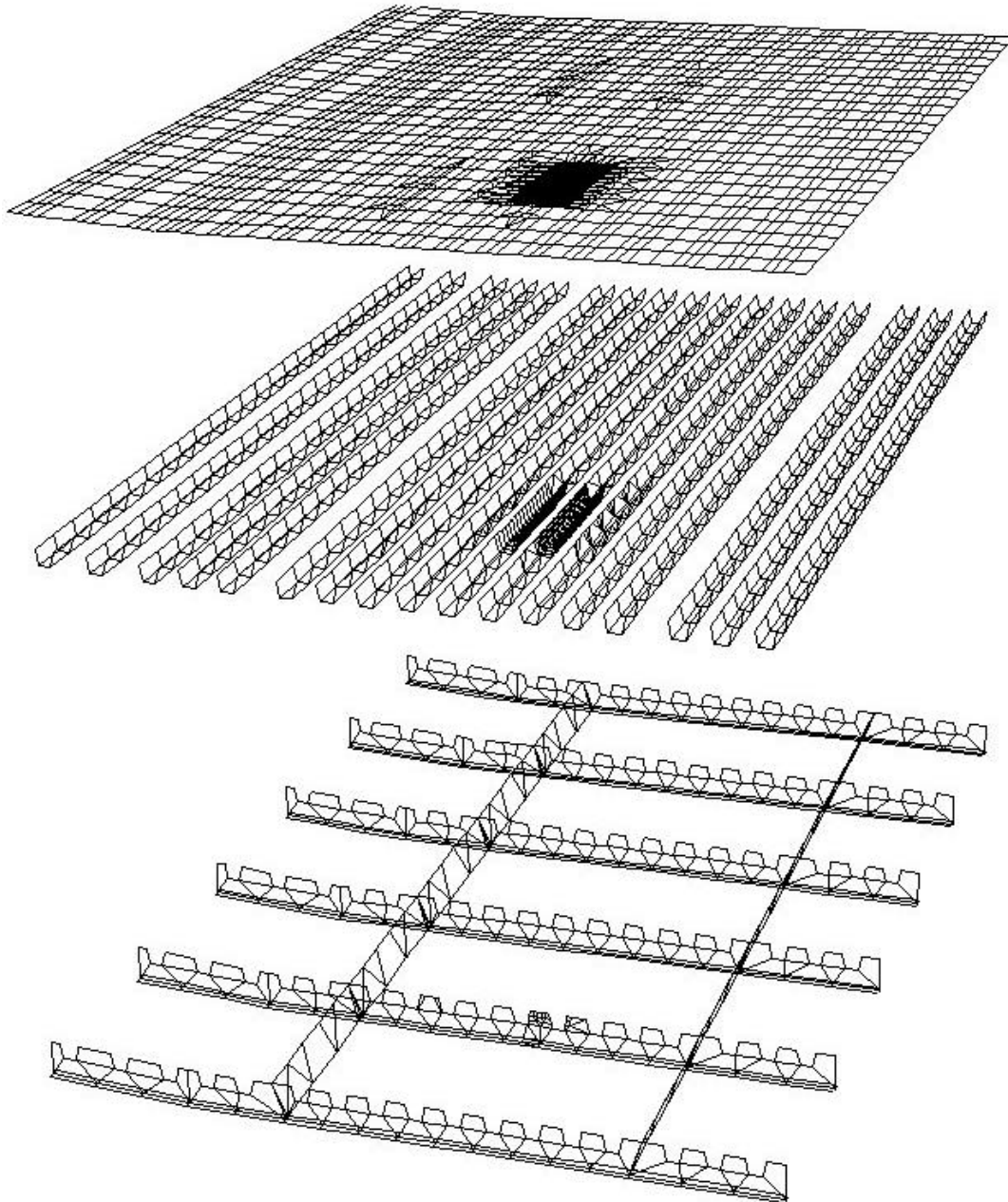
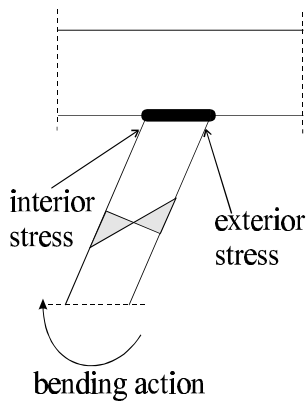


Fig. 3.1 FEM mesh of the bridge deck

It is seen from the results, that maximum stresses are achieved by placing the wheel around the rib mid-span. An other observation: the bending stresses in the rib wall under a certain wheel are virtually unaffected by the other wheels (they are very localized).



Position	Node # for σ_{\min}	Node # for σ_{\max}	σ_{\min} [MPa]	σ_{\max} [MPa]
1	1335	1399	-37.3 (+31.2)	+42.1 (-47.4)
2	1335	1337	-34.8 (+24.2)	+30.7 (-31.5)
3	1335	1328	-19.5 (+17.4)	+29.3 (-37.3)
4	1809	1860	-8.4 (-2.1)	+25.5 (-24.4)
5	1797	1860	-15.4 (+4.9)	+17.6 (-18.8)
6	1824	1754	-9.2 (+6.4)	+31.1 (-21.1)
7	1654	1754	-20.3 (+15.0)	+24.1 (-13.9)
8	1643	1692	-19.8 (+9.4)	+14.8 (-8.0)
9	1790	1754	-7.7 (-2.4)	+25.2 (-13.7)

Tab. 3.1 Min. and max. stresses from fatigue load model 3

Based on the observations made after the first stress analysis, the following simplifications were introduced when defining fatigue load model 4:

1. Only one wheel was placed on the deck because of the extremely localized nature of the bending stresses in the ribs,
2. The wheels were placed around rib mid-span with two different lateral positions.

3.3 Fatigue assessment based on equivalent constant amplitude

Because of the localized nature of the stresses in the rib walls, the stress history in the studied weld depends almost entirely on the specific wheel passing over it. Therefore, the most conservative assumption can be made by supposing the *two worst possibilities*:

1. the stresses grow from zero to the maximum possible *tensile* stress, then decrease to zero as the wheel passes (50% of the cases).
2. the stresses grow from zero to the maximum possible *compressive* stress, then decrease to zero as the wheel passes (50% of the cases).

As shown in part 3.2, the maximum possible tensile and compressive stresses obtained from fatigue load model 3 were the following: $\sigma_{\min} = -37.3$ MPa and $\sigma_{\max} = 42.1$ MPa. The reference stress range can be assumed to be the average of their absolute values: $\Delta\sigma_p = |\sigma_{\max} - \sigma_{\min}| / 2 = 39.7$ MPa. According to Fig. 9.4 of ENV 1993-2, 1996, the maximum value of the *damage equivalence factor* for road bridges is: $\lambda_{\max} = 1.7$ (the span of the ribs is equal to the cross girder spacing: 3.00 m). The fatigue load models already include a dynamic load amplification corresponding to a good roughness of the pavement. The *equivalent constant amplitude stress range for 2 million cycles* will be: $\Delta\sigma_{E2} = 67.5$ MPa according to Eq. 3. Since we may assume a fail-safe design, local failure will occur without severe consequences. Therefore, according to Eurocode 3, the partial safety factor for fatigue strength is: $\gamma_{Mf} = 1.0$. The same standard gives the value of the partial safety factor for fatigue loading as $\gamma_{Ff} = 1.0$. According to Tab. 9.8.5 of Annex N, ENV 1993-2, 1996, the trapezoidal stiffener to deck plate welds with full penetration weld fall into Detail Category 71, which means that the reference value of the fatigue strength at 2 million cycles is: $\Delta\sigma_c = 71$ MPa. Substituting the values into Eq. 2:

$$67.5 \text{ MPa} < 71 \text{ MPa.}$$

The fatigue assessment criterion is fulfilled, therefore the structural detail may be considered safe from the point of view of fatigue failure during *100 years of service*.

3.4 Fatigue assessment based on linear damage accumulation

Organizing the results of the model's stress analysis for different locations of the three types of wheels, and assuming that the maximum tensile stresses occur 50% of the time, while maximum compressive stresses occur the other 50% of the time; and considering the different axle weights and the traffic mixes predicted for the route (assuming traffic category 2: "Roads and motorways with medium flow rates of lorries", 500 thousand lorries per year), we obtain the following stress spectrum for one year (Fig. 3.2):

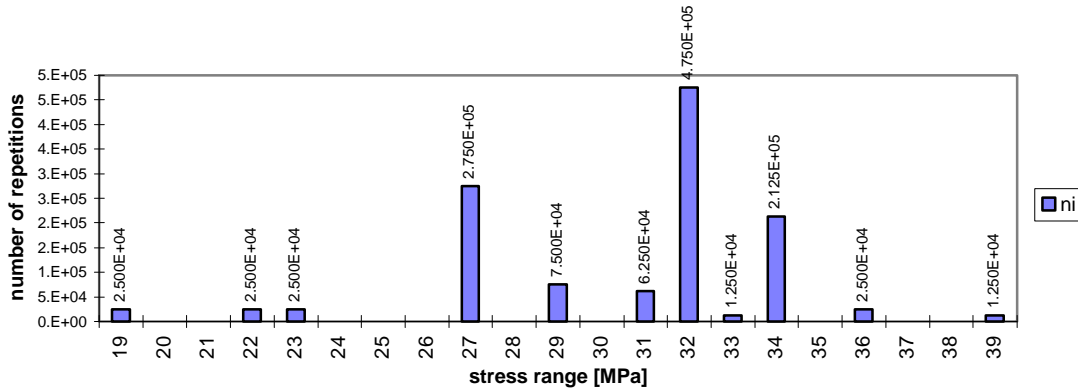


Fig. 3.2 Stress spectrum for one year

The fatigue strength curve for Category 71 can be expressed as the following - see Eq. 1:

$$N = \frac{a}{\Delta\sigma^3} \text{ if } \Delta\sigma \geq \Delta\sigma_D \quad \text{and} \quad N = \frac{b}{\Delta\sigma^5} \text{ if } \Delta\sigma \leq \Delta\sigma_D \quad (5)$$

Substituting $N=2 \times 10^6$, into Eq. 5 we must obtain the reference value $\Delta\sigma_c = 71.0$ MPa, so $a = 7.16 \times 10^{11}$. At $N = 5 \times 10^6$, the logarithmic slope changes from 3 to 5, at the value $\Delta\sigma_D = 52.31$ MPa. From Eq. 5, $b = 1.96 \times 10^{15}$. Using these values, the fatigue lives N_i and the damage $D_i = n_i/N_i$ can be computed for each stress range $\Delta\sigma_i$. The results are summarized in Tab. 3.2. It can be seen that the **cumulative damage** over one year is: $D_{\text{year}} = 0.01797$. Therefore, assuming the same traffic every year, fatigue failure can be expected when accumulated damage reaches 1.0: **Life** = $1/D_{\text{year}} = 55.65$ years.

$\Delta\sigma_i$	i	n_i	m	a or b	N_i	D_i
19	1	2.500E+04	5	1.96E+15	7.916E+08	3.16E-05
22	4	2.500E+04	5	1.96E+15	3.803E+08	6.57E-05
23	5	2.500E+04	5	1.96E+15	3.045E+08	8.21E-05
27	9	2.750E+05	5	1.96E+15	1.366E+08	0.002013
29	11	7.500E+04	5	1.96E+15	9.556E+07	0.000785
31	13	6.250E+04	5	1.96E+15	6.846E+07	0.000913
32	14	4.750E+05	5	1.96E+15	5.841E+07	0.008132
33	15	1.250E+04	5	1.96E+15	5.008E+07	0.00025
34	16	2.125E+05	5	1.96E+15	4.314E+07	0.004926
36	18	2.500E+04	5	1.96E+15	3.241E+07	0.000771
39	21	1.250E+04	5	1.96E+15	3.304E+10	3.78E-07
TOTAL		1.225E+06				0.01797

Tab. 3.2 Computing damage accumulation

4. CONCLUSIONS

It can be seen from looking at the stress analysis results, that the *local bending stresses* are dominant in rib-to-deckplate welds, if stresses *normal to the weld axis* are to be considered. Stresses from the orthotropic deck action and the main girder effect may be ignored, because they would cause mainly *longitudinal stresses* in the ribs without noticeable bending. The localized nature of the bending stresses is so pronounced, that it is enough to apply just one wheel above the weld and ignore the effect of the other wheels.

In case of full penetration butt-welds, normal stresses in the weld can be obtained simply from the extreme fiber stresses in the rib walls. However, analysis of partial penetration butt welds or fillet welds would require a *2D model of the weld* of plane strain plate elements.

Performing two different fatigue checks based on the *S-N curves* and fatigue load models 3 and 4 of *Eurocode 3*, it can be noted that they give quite different results: the first check gives the fatigue life of the component as being over 100 years (using the maximum value of the damage equivalence factor), while the second check gives a fatigue life of 55 years. The result of the second check could be greatly improved by considering Paragraph 6 of Chapter 4.6.1, (ENV 1991-3, 1993): "... when the *transverse location of the vehicles* is significant for the studied effects, statistical distribution of this transverse location should be considered". This would significantly change the stress spectrum and increase fatigue life.

5. ACKNOWLEDGEMENTS

The author wishes to acknowledge the financial support of the OTKA project #T023378.

6. REFERENCES

- Bannantine, A.; Corner, J. J. and Handrock, J. L. (1990), "Fundamentals of metal fatigue analysis", Prentice Hall, Englewood Cliffs.
- Davoli, P. (1997), "Principles of current methodologies in fatigue design of metallic structures", *Lecture notes for the advanced course on "High-cycle metal fatigue in the context of mechanical design"*, Sept. 8-12, 1997, CISM, Udine.
- ENV 1991-3 (1993), "Basis of design and actions on structures, Part 3: Traffic loads on bridges".
- ENV 1993-1-1 (1992), "Design of Steel Structures, Part 1.1: General Rules and Rules for Buildings".
- ENV 1993-2 (1996), "Design of steel structures, Part 2: Steel bridges".
- Forsyth (1969) "The physical basis of metal fatigue", Blackie & Son Ltd, London.
- Kiss, K.(1997): "Fatigue of Metallic Structures", *A chapter of Refurbishment in Steel as an Environmentally Friendly Activity*, Multimedia CD-ROM prepared by Tempus JEP 09524, Budapest.
- Maddox, S. J. (1991), "Fatigue Strength of Welded Structures", 2nd Ed, Woodhead Publishing Ltd., Cambridge CB1 6AH, England.